

SCIENTIFIC REPORTS

OPEN

Tonoplast-localized nitrate uptake transporters involved in vacuolar nitrate efflux and reallocation in *Arabidopsis*

Ya-Ni He^{1,2,3}, Jia-Shi Peng¹, Yao Cai^{1,2}, De-Fen Liu^{1,2}, Yuan Guan^{1,3}, Hong-Ying Yi¹ & Ji-Ming Gong¹ 

A great proportion of nitrate taken up by plants is stored in vacuoles. Vacuolar nitrate accumulation and release is of great importance to nitrate reallocation and efficient utilization. However, how plants mediate nitrate efflux from vacuoles to cytoplasm is largely unknown. The current study identified NPF5.11, NPF5.12 and NPF5.16 as vacuolar nitrate efflux transporters in *Arabidopsis*. Histochemical analysis showed that NPF5.11, NPF5.12 and NPF5.16 were expressed preferentially in root pericycle cells and xylem parenchyma cells, and further analysis showed that these proteins were tonoplast-localized. Functional characterization using cRNA-injected *Xenopus laevis* oocytes showed that NPF5.11, NPF5.12 and NPF5.16 were low-affinity, pH-dependent nitrate uptake transporters. In *npf5.11 npf5.12 npf5.16* triple mutant lines, more root-fed ¹⁵NO₃⁻ was translocated to shoots compared to the wild type control. In the NPF5.12 overexpression lines, proportionally less nitrate was maintained in roots. These data together suggested that NPF5.11, NPF5.12 and NPF5.16 might function to uptake nitrate from vacuoles into cytosol, thus serving as important players to modulate nitrate allocation between roots and shoots.

Nitrate is the major nitrogen source for most plants, especially those grown in aerobic soil conditions¹. Once taken up from soil, nitrate is either assimilated or stored in vacuoles. As the largest organelle in fully expanded plant cells, vacuoles are identified as the major nitrate storage pools and contain up to 90% of the total cellular nitrate^{2,3}. However, vacuolar nitrate is not readily accessible to NR (nitrate reductase), thus it has to be reallocated for metabolic use when necessary^{4,5}. Vacuolar nitrate release helps to maintain the relative steady level of cytosolic nitrate when external nitrogen supply was limited^{6,7}. During the dark-to-light transition, nitrate remobilization from vacuoles was also observed to comply with the new steady state caused by the increased NR activity⁴. Therefore, vacuolar nitrate and its remobilization are important for the regulation of nitrogen assimilation and nitrogen use efficiency^{5,8,9}.

Transport across the tonoplast is energized by the vacuolar H⁺-ATPase (V-ATPase) and the vacuolar H⁺-pyrophosphatase (V-PPase), which create the proton gradient and the membrane potential^{10–12}. For nitrate, its accumulation in vacuoles is probably mediated by the nitrate/proton antiporter machinery^{13–16} and the nitrate/proton symport system may serve to remobilize vacuolar nitrate^{16–18}. However, only a few tonoplast localized nitrate transporters have been identified up to date. AtCLCa and AtNRT2.7 are two transporters responsible for nitrate accumulation in vacuoles^{19–21}. AtCLCa was a tonoplast localized 2NO₃⁻/1 H⁺ antiporter expressed in both shoots and roots^{20,22}. Disruption of AtCLCa led to approximately 50% decrease of vacuolar nitrate, suggesting an important role for AtCLCa in vacuolar nitrate accumulation^{19,20}. AtNRT2.7, however, was a tonoplast localized transporter expressed exclusively in seeds, which regulated the kinetics of seed germination by affecting nitrate storage in seed vacuoles²¹. AtCLCc was also supposed to be involved in vacuolar nitrate accumulation, because

¹National Key Laboratory of Plant Molecular Genetics and National Center for Plant Gene Research (Shanghai), CAS Center for Excellence in Molecular Plant Sciences, Institute of Plant Physiology and Ecology, Shanghai Institutes for Biological Sciences, Chinese Academy of Sciences, Shanghai, 200032, People's Republic of China. ²University of Chinese Academy of Sciences, Beijing, 100049, China. ³Forestry and Fruit Tree Research Institute, Shanghai Academy of Agricultural Sciences, Shanghai, 201403, China. Correspondence and requests for materials should be addressed to J.-M.G. (email: jmgong@sibs.ac.cn)

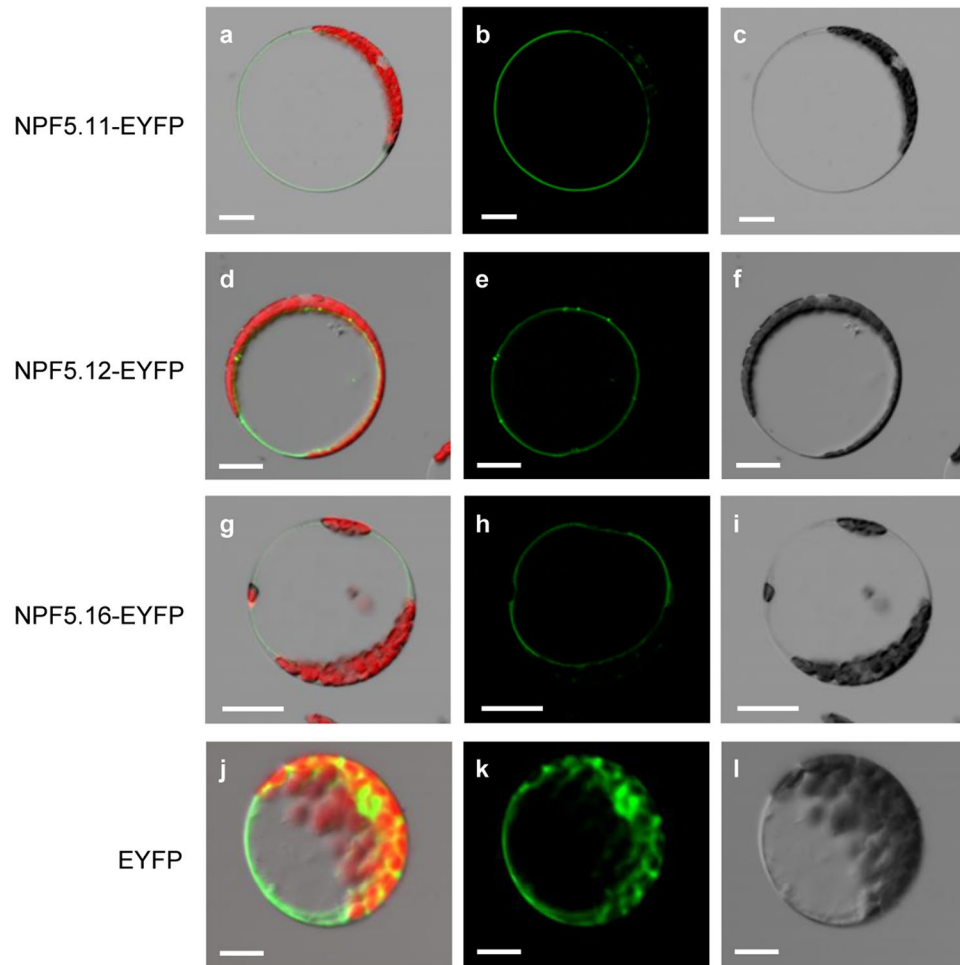


Figure 1. Subcellular localization of NPF5.11, NPF5.12 and NPF5.16. *NPF5.11-EYFP* (a–c), *NPF5.12-EYFP* (d–f), *NPF5.16-EYFP* (g–i) or *EYFP* (j–l) was driven by the cauliflower mosaic virus 35 S promoter and transiently expressed in *Arabidopsis* mesophyll protoplasts. Overlap images of EYFP (green) and chlorophyll (red) fluorescence (a,d,g,j), EYFP fluorescence (b,e,h,k), and bright-field (c,f,i,l) images are shown. Bars = 20 μ m.

it was tonoplast localized and the related mutants showed lower nitrate contents^{22,23}. Regarding nitrate efflux from vacuoles, however, indirect evidences imply that AtCLCb and OsNPF7.2 might get involved, as they both were tonoplast-localized, and heterologous expression in *Xenopus laevis* oocytes indicated that they mediated nitrate uptake, but no evidence showed that functional disruption of these genes led to nitrate accumulation in vacuoles^{24,25}. AtCLCa was also implied to get involved in vacuolar nitrate efflux, because it mediated anion homeostasis in stomata movement²⁶, while nitrate is one of the anions contributing to stomatal movement^{27,28}.

In the current study, three tonoplast-localized NRT1/NPF family members NPF5.11, NPF5.12 and NPF5.16 were identified by bioinformatics analysis, and functional characterization was performed. Our data suggested that these three transporters were all tonoplast localized, and mediated nitrate uptake in a pH-dependent low-affinity manner when heterologously expressed in oocytes. Further analysis indicated that they possibly modulated nitrate allocation between roots and shoots via vacuolar nitrate release.

Results

Tonoplast Localization of NPF5.11, NPF5.12 and NPF5.16. Based on previous studies about vacuole proteome²⁹, we targeted NPF5.12 and its close homologs NPF5.11 and NPF5.16, members of NRT1/NPF family³⁰, as candidate transporters for vacuolar nitrate transport. NPF5.11, NPF5.12 and NPF5.16 were predicted to contain 11, 12, 10 transmembrane domains (<http://www.cbs.dtu.dk/services/TMHMM/>), respectively. To investigate the subcellular localization of NPF5.11, NPF5.12 and NPF5.16, *NPF5.11-EYFP*, *NPF5.12-EYFP* and *NPF5.16-EYFP* driven by the cauliflower mosaic virus 35 S promoter were transiently expressed in *Arabidopsis* mesophyll protoplast. The yellow fluorescence signals of NPF5.11-EYFP (Fig. 1a–c), NPF5.12-EYFP (Fig. 1d–f) and NPF5.16-EYFP (Fig. 1g–i) were detected in the membrane around the large central vacuole. Similar results were obtained by transiently expressing these fusion proteins in onion epidermal cells, verifying that NPF5.11, NPF5.12 and NPF5.16 were tonoplast localized (Supplementary Fig. S1).

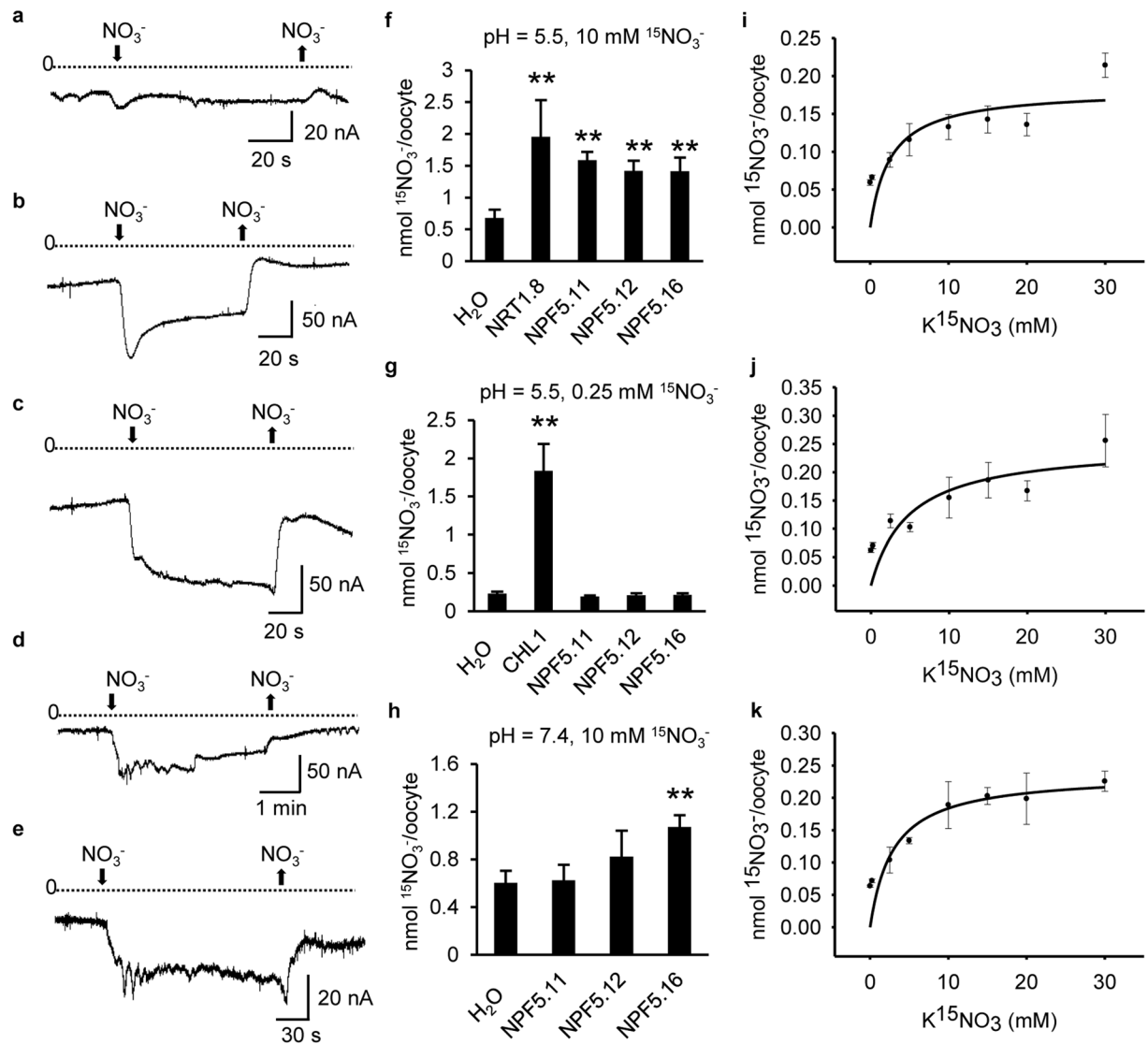


Figure 2. Functional characterization of NPF5.11, NPF5.12 and NPF5.16 in oocytes. (a–e) Currents elicited in oocytes injected with H₂O (a), *CHL1* cRNA (b), *NPF5.11* cRNA (c), *NPF5.12* cRNA (d) or *NPF5.16* cRNA (e). Oocytes were voltage clamped at -60 mV and representative inward currents elicited by 10 mM NO_3^- at pH 5.5 were recorded. (f–h) Nitrate uptake activity in oocytes injected with H₂O, *NPF5.11* cRNA, *NPF5.12* cRNA, *NPF5.16* cRNA, *NRT1.8* cRNA or *CHL1* cRNA. Oocytes were incubated with 10 mM $^{15}\text{NO}_3^-$ at pH 5.5 (f), 0.25 mM $^{15}\text{NO}_3^-$ at pH 5.5 (g) or 10 mM $^{15}\text{NO}_3^-$ at pH 7.4 (h) for 12 h. Values are means \pm SD ($n = 8$ –12). Asterisks indicate difference at $P < 0.01$ (**) compared with the H₂O-injected oocytes by Student's *t*-test. (i–k) Uptake kinetics of NPF5.11 (i), NPF5.12 (j) and NPF5.16 (k). Oocytes injected with *NPF5.11* cRNA (i), *NPF5.12* cRNA (j) or *NPF5.16* cRNA (k) were incubated with indicated concentrations of $^{15}\text{NO}_3^-$ at pH 5.5 for 1.5 h, and the ^{15}N contents were determined. Values are means \pm SD ($n = 6$ –12). The K_m was calculated by fitting to the Michaelis-Menten equation using a nonlinear least squares method in the SigmaPlot program. The K_m was 2.57 mM, 4.84 mM, or 2.91 mM for NPF5.11, NPF5.12 or NPF5.16, respectively.

NPF5.11, NPF5.12 and NPF5.16 are pH-dependent Low-Affinity Nitrate Transporters. Given that *Xenopus laevis* oocytes did not contain vacuoles, we firstly tested the expression and localization of NPF5.11, NPF5.12 and NPF5.16 in oocytes. As a well-documented nitrate transporter³¹, NRT1.8 fused with GFP was used as a positive control and its fluorescence was detected at the rim of oocytes (Supplementary Fig. S2). Likewise, NPF5.11-EYFP, NPF5.12-EYFP and NPF5.16-EYFP fusion proteins could express in plasma membrane of oocytes though they were tonoplast localized transporters in *Arabidopsis*, indicating that we could use oocytes to explore the function of NPF5.11, NPF5.12 and NPF5.16 (Supplementary Fig. S2).

Electrophysiological analysis using cRNA-injected oocytes were performed to test whether NPF5.11, NPF5.12 and NPF5.16 could use nitrate as substrate. After 2 days of incubation, oocytes were voltage clamped at -60 mV and perfused with 10 mM nitrate at pH 5.5. Compared with water-injected oocytes (Fig. 2a), a larger inward current was induced by CHL1-injected oocytes (Fig. 2b), as reported before³². NPF5.11-, NPF5.12- or

NPF5.16-injected oocytes also induced inward currents (Fig. 2c–e), indicating that they were electrogenic transporters using nitrate as the substrate.

Nitrate transport activities of NPF5.11, NPF5.12 and NPF5.16 were further confirmed by analyzing $^{15}\text{NO}_3^-$ uptake activity. NPF5.11-, NPF5.12-, NPF5.16- or NRT1.8-injected oocytes showed enhanced $^{15}\text{NO}_3^-$ uptake activity when incubated with 10 mM $^{15}\text{NO}_3^-$ at pH 5.5, compared with water-injected oocytes (Fig. 2f). However, NPF5.11-, NPF5.12- or NPF5.16-injected oocytes almost did not uptake $^{15}\text{NO}_3^-$ when assayed with 0.25 mM $^{15}\text{NO}_3^-$ at pH 5.5, while CHL1-injected oocytes still showed high uptake activity (Fig. 2g). In addition, as expected for proton-coupled transporters, $^{15}\text{NO}_3^-$ uptake activities of NPF5.11-, NPF5.12- or NPF5.16-injected oocytes at pH 7.4 were much lower than those at pH 5.5, comparable with the negative control (Fig. 2h). It is worth mentioning that NPF5.11, NPF5.12 and NPF5.16 did not efflux nitrate from oocytes under pH 5.5 or pH 7.4 (Supplementary Fig. S3).

To further determine the uptake affinity of NPF5.11, NPF5.12 and NPF5.16, uptake activity of NPF5.11-, NPF5.12- or NPF5.16-injected oocytes at pH 5.5 was measured using different concentrations of $^{15}\text{NO}_3^-$ ranging from 0.25 mM to 30 mM as substrates. The K_m for nitrate was calculated by fitting to the Michaelis-Menten equation, and was estimated as 2.57 mM, 4.84 mM, 2.91 mM respectively for NPF5.11, NPF5.12 and NPF5.16 (Fig. 2i–k). Taken together, these results suggested that NPF5.11, NPF5.12 and NPF5.16 were pH-dependent low-affinity nitrate transporters.

NPF5.11, NPF5.12 and NPF5.16 are mainly expressed in vascular stele of roots and leaves. The tissue localization of genes could provide hint for their physiological role. To elucidate the expression pattern of *NPF5.11*, *NPF5.12* and *NPF5.16*, promoter-GUS (β -glucuronidase) reporter analysis was performed. The promoter region of *NPF5.11*, *NPF5.12* and *NPF5.16* were used for driving the expression of GUS in Columbia (Col-0). As shown in Fig. 3, *NPF5.11*, *NPF5.12* and *NPF5.16* had a similar expression pattern, expressing in both shoots and roots. In shoots, they were mainly expressed in leaf veins while the mesophyll cells were also stained (Fig. 3a,e,i). In roots, GUS activity was detected in root vascular stele (Fig. 3b,f,j). Cross-sections of young seedling roots showed that *NPF5.11_{pro}::GUS*, *NPF5.12_{pro}::GUS* and *NPF5.16_{pro}::GUS* were expressed in pericycle cells and parenchyma cells, and *NPF5.11_{pro}::GUS* was also expressed in the phloem (Fig. 3c,d,g,h,k,l).

The expression patterns of these three genes in adult plant were further investigated by qRT-PCR analysis. *NPF5.11*, *NPF5.12* and *NPF5.16* all showed high expression in root while the expression in flower and stem was quite low (Fig. 3m,n,o). The expression of *NPF5.12* in old leaves was higher than that in young leaves, while *NPF5.16* was preferentially expressed in young leaves (Fig. 3n,o).

More nitrate is translocated to shoots in triple mutant. Considering the tonoplast localization (Fig. 1) and pH-dependent nitrate uptake (Fig. 2), we proposed that NPF5.11, NPF5.12 and NPF5.16 might be responsible for uptaking nitrate from vacuole (pH 5.5³³) to cytoplasm in *Arabidopsis*. To test this hypothesis, we generated several lines of their single, double, and even triple mutants (Supplementary Figs S4,S6,S7). Note that only double mutant lines of *npf5.12 npf5.16* were generated because *NPF5.11* and *NPF5.12* were tightly linked in *Arabidopsis* genome and *npf5.11* mutant lines were in Ws background. Given vacuolar nitrate efflux is supposed to be enhanced when nitrogen is limited, we firstly analyzed the nitrate contents in leaves and roots in these mutants under both control condition and nitrogen-starved condition. As shown in Supplementary Figs S5, S6 and S7, no obvious difference was observed between the wild type control and all the mutants. However, when they were fed with $^{15}\text{NO}_3^-$, the ratio of ^{15}N concentration in shoots against that in roots (shoot/root) was higher in triple mutant lines than in the wild type (Fig. 4a, Supplementary Fig. S8), while no significant difference was observed between the single mutant lines and the wild type (Supplementary Fig. S9). These results suggested that more $^{15}\text{NO}_3^-$ was translocated to shoots in triple mutants, while our data also indicated that the root uptake capacity of triple mutant lines was not affected (Fig. 4b).

Root nitrate content is reduced in NPF5.12 overexpression lines. To further investigate the function of NPF5.11, NPF5.12 and NPF5.16, the overexpression lines of *NPF5.11*, *NPF5.12* and *NPF5.16* under the control of 35S promoter were generated (Fig. 5a,b) and the nitrate content was analyzed (Fig. 5c, Supplementary Figs S10, S11). The result showed that nitrate contents in roots of *NPF5.12* overexpression lines were lower than that of wild type under nitrogen-starved condition (Fig. 5c). This observation was not found in *NPF5.11* and *NPF5.16* overexpression lines (Supplementary Fig. S11). One explanation could be that NPF5.11 and NPF5.16 might require other components to function properly in planta.

Discussion

Significant progresses have been made in clarifying the nitrate uptake and transport in *Arabidopsis* by the characterization of the transporters in NRT1/NPF, NRT2, CLC and SLAC/SLAH families³⁴. However, our current knowledge about nitrate transport across the tonoplast is quite limited though the significance of this process is widely recognized.

The transporters responsible for vacuolar nitrate efflux should be tonoplast-localized and uptake nitrate toward cytoplasm. Our data suggested that NPF5.11, NPF5.12 and NPF5.16 were localized in tonoplast in *Arabidopsis* (Fig. 1) and plasma membrane in *Xenopus laevis* oocytes (Supplementary Fig. S2), and in oocytes they could elicit inward currents by external nitrate and uptake nitrate in a pH dependent way (Fig. 2). When these results were assigned to the topology of the plant tonoplast, the inward currents might represent NO_3^-/H^+ efflux from the vacuole to the cytoplasm²⁴, because the external medium for oocytes corresponds to the vacuole in planta^{35,36} and the pH of vacuole in *Arabidopsis* is about 5.5^{33,37}. Thus we speculated that NPF5.11, NPF5.12 and NPF5.16 were responsible for vacuolar nitrate release in *Arabidopsis*.

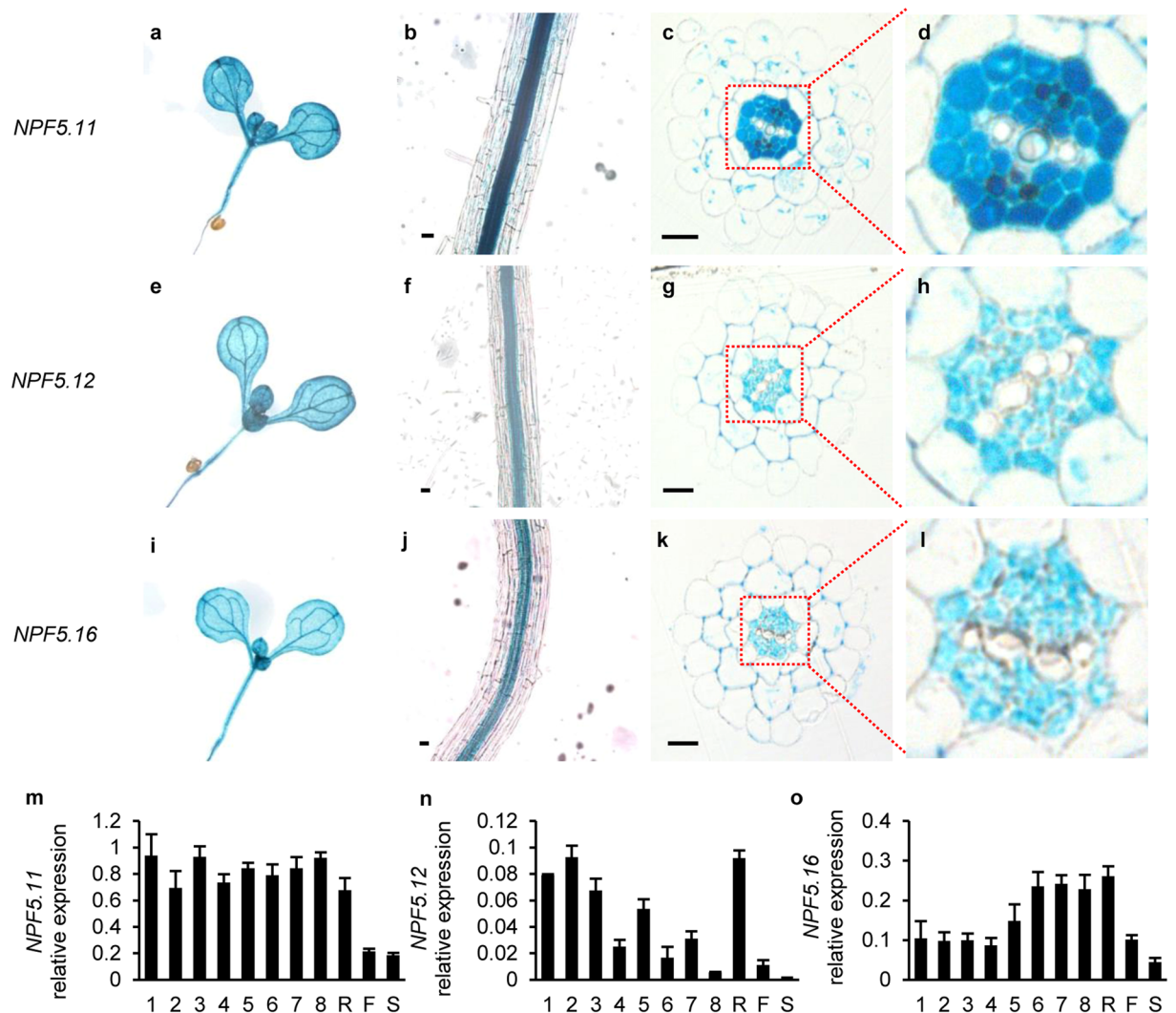


Figure 3. *NPF5.11*, *NPF5.12* and *NPF5.16* are preferentially expressed in vascular tissues. Histochemical localization of GUS activity in *NPF5.11_{pro}::GUS* transgenic plants (a–d), *NPF5.12_{pro}::GUS* transgenic plants (e–h) and *NPF5.16_{pro}::GUS* transgenic plants (i–l). The expression patterns of *NPF5.11*, *NPF5.12* and *NPF5.16* were determined in whole-mount seedlings (a,e,i), seedling roots (b,f,j) or cross-sectioned seedling roots (c,d,g,h,k,l). (m,n,o) Transcript expression of *NPF5.11* (m), *NPF5.12* (n) and *NPF5.16* (o) in 28 d old plants. 1–8 indicated leaf positions arranged according to leaf ages (old to young); R, root; F, flower; S, stem. Data were normalized to that of *SAND*. Values are means \pm SD, n = 3. Bars = 10 μ m.

Considering that *NPF5.11*, *NPF5.12* and *NPF5.16* are predominantly expressed in vacuole membrane of pericycle cells and xylem parenchyma cells in roots (Figs 1, 3). We proposed that they might be involved in the regulation of nitrate long-distance transport by modulating the vacuolar sequestration capacity (VSC) of nitrate in roots. Relationship between VSC and long-distance transport of metals in plant have been well documented³⁸, and accumulating evidences indicated that VSC of essential anions including sulfate and nitrate also regulated their long-distance transport^{39,40}. The vacuolar sulfate efflux transporters *SULTR4;1* and *SULTR4;2* played an essential role in delivering sulfate to the xylem vessels by balancing storage and turnover of sulfate in the root vacuoles³⁹. While Han *et al.*, found that the decreased VSC of nitrate in roots would enhance nitrate transport to shoots and contribute to a higher nitrogen use efficiency (NUE)⁴⁰. Our hypothesis about the physiological role of *NPF5.11*, *NPF5.12* and *NPF5.16* was supported by the observation that more proportion of $^{15}\text{NO}_3^-$ was translocated to shoots in triple mutant lines (Fig. 4) and overexpression of *NPF5.12* resulted in a lower nitrate contents in roots (Fig. 5c). In the triple mutant lines, root VSC increased but not too much was available to newly absorbed nitrate due to the impaired nitrate efflux from vacuoles, resulting in less vacuolar nitrate sequestration and the consequent enhancement of $^{15}\text{NO}_3^-$ long-distance transport to shoots when fed with $^{15}\text{NO}_3^-$ for a short time (30 min). In *NPF5.12* overexpression lines, the overall nitrate contents in roots decreased because of the lower VSC of nitrate, thus leading to the higher S/R ratios in the overexpression lines (Fig. 5c, Supplementary Fig. S10b).

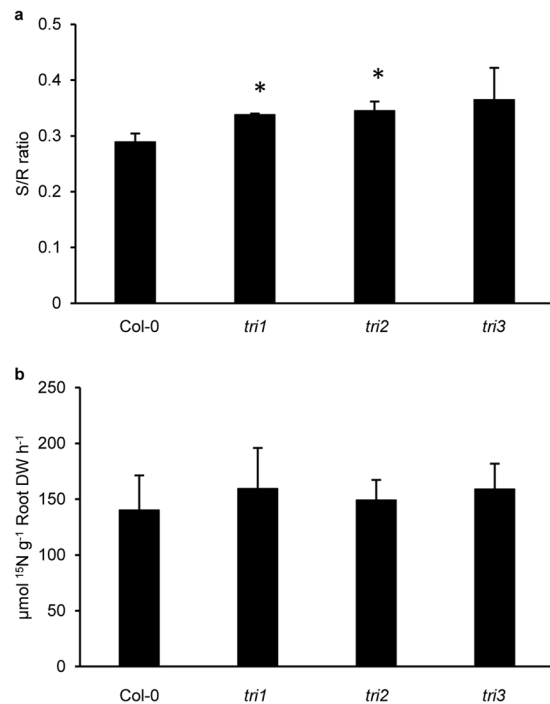


Figure 4. Root-to-shoot nitrate transport enhanced in the triple mutant plants *npf5.11 npf5.12 npf5.16*. Plants were grown in hydroponics for 28 days and treated with 2.25 mM K^{15}NO_3 for 30 min. ^{15}N contents in shoots and roots were analyzed. ^{15}N concentration ratio between shoots and roots (S/R ratio, **a**) and root uptake activity (**b**) were determined. Values are means \pm SD, $n = 3$. Asterisks indicate difference between wild type and triple mutant lines at $P < 0.05$ (*) by Student's *t*-test.

No significant difference of nitrate contents was detected between all the mutants and wild type under various growth conditions we tested (Supplementary Figs S5, S6, S7). We proposed that there might be other transporters or channels that function redundantly with NPF5.11, NPF5.12 and NPF5.16, as the reutilization of vacuolar nitrate is crucial to environmental adaption for plants. The speculation is according with the observation that more $^{15}\text{NO}_3^-$ was translocated to shoots in triple mutant but not in single mutant. Similarly, no obvious changes in nitrate allocation was observed in mutants of *AtCLCb* or *OsNPF7.2*^{24,25}. In addition, considering their specific tissue localization in roots (Fig. 3), we speculated that physiological effect of NPF5.11, NPF5.12 and NPF5.16 in nitrate allocation might be more noticeable specifically in pericycle cells and parenchyma cells. Thus more definitive evidences are needed in the future to demonstrate the working model for vacuolar nitrate efflux.

Methods

Plant Materials and Growth Conditions. *Arabidopsis* (*Arabidopsis thaliana*) ecotype Col-0 or Ws was used as the wild-type control. The *Arabidopsis* T-DNA mutant lines *npf5.11-1* (FLAG_493A07) and *npf5.11-2* (FLAG_592C02) were ordered from INRA (National Institute for Agricultural Research)⁴¹; *npf5.12-1* (GABI_810C10) was ordered from NASC (European Arabidopsis Stock Centre)⁴²; *npf5.12-2* (CS871745), *npf5.16-1* (SALK_152449C) and *npf5.16-2* (SALK_200474C) were ordered from ABRC (Arabidopsis Biological Resource Center)^{43,44}. Homozygous mutant plants were screened by PCR⁴⁵. The *npf5.12 npf5.16* double mutant lines of were generated by crossing *npf5.12* and *npf5.16* and identified by PCR. The double mutant *npf5.12 npf5.16* was further transformed with CRISPR/Cas9 system to generate the triple mutant *npf5.11 npf5.12 npf5.16*, using two different target sequences⁴⁶. The double mutant lines used for transformation were: *tri1, npf5.12-1 npf5.16-2; tri2, npf5.12-1 npf5.16-1; tri3, npf5.12-2 npf5.16-1*. The CRISPR-Cas9 T-DNA was not existent in triple mutants by Cas9 PCR confirming⁴⁷. The primers used in these assays are listed in Supplemental Table S1.

Arabidopsis plants were grown in quarter-strength hydroponic solution at 22 °C with 16-h-light/8-h-dark cycles as described⁴⁸. Plants were grown to 3-4 weeks old and then were treated with nitrogen-starved nutrient solution by replacing KNO_3 and $\text{Ca}(\text{NO}_3)_2$ with KCl and CaCl_2 as indicated time.

Functional Analysis of NPF5.11, NPF5.12 and NPF5.16 in *Xenopus laevis* Oocytes. cDNA fragments of targeted genes were recovered by restriction digestion and then subcloned into the oocyte expression vector pOO2⁴⁹. cRNA was synthesized using the Ambion mMessage mMachine kit according to the manufacturer's manual. Oocytes were isolated and injected with 50 ng cRNA as described previously⁵⁰. *CHL1* cRNA or *NRT1.8* cRNA injected oocytes were used as positive control and water-injected oocytes were used as negative control. Oocytes were incubated in a ND-96 Ringer solution for 2 days as described³¹. Voltage clamp recordings were initiated in a bath solution containing 230 mM mannitol, 0.15 mM CaCl_2 , and 10 mM MES/Tris, pH 5.5⁵¹. Nitrate uptake or efflux assays with $^{15}\text{NO}_3^-$ were performed as described^{50,52,53} using a continuous-flow isotope

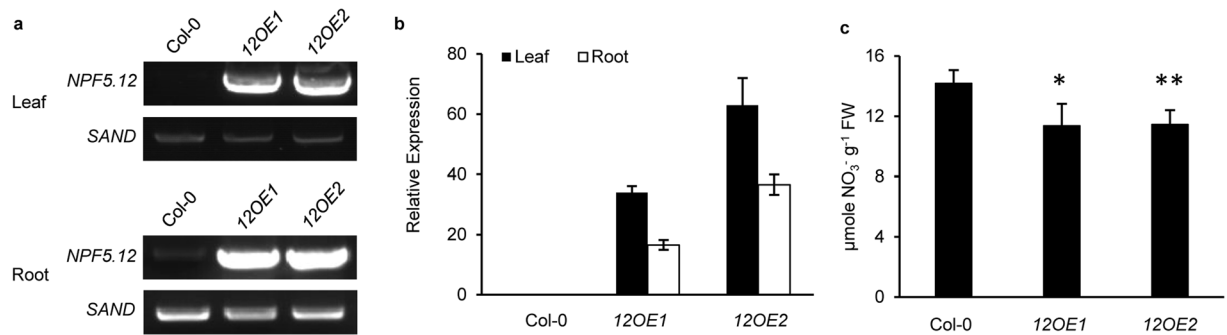


Figure 5. Decreased nitrate accumulation in roots of *NPF5.12* overexpression lines. **(a,b)** Identification of *NPF5.12* overexpression lines by RT-PCR **(a)** and quantitative PCR analysis **(b)**. **(c)** 24 days old hydroponically grown plants were subjected to nitrogen-starvation for 30 h, then roots were sampled and nitrate contents were determined by HPLC. *12OE1* and *12OE2* were two independent *NPF5.12* overexpression lines. Values are means \pm SD, $n = 5-7$. Asterisks indicate difference between wild type and overexpression lines at $P < 0.05$ (*) and $P < 0.01$ (**) by Student's *t*-test.

ratio mass spectrometer coupled to a carbon nitrogen elemental analyzer (Vario EL III/Isoprime; Elementar). Uptake kinetics assays were performed as described⁵⁴.

EYFP Fusion and Subcellular Localization. The amplified *NPF5.11*, *NPF5.12* and *NPF5.16* cDNA fragments were cloned in frame in front of *EYFP* in the vector 35S::*EYFP*/PA7, resulting in the *NPF5.11-EYFP*, *NPF5.12-EYFP* and *NPF5.16-EYFP* constructs under the control of the 35 S promoter. The resulted constructs were transiently expressed in *Arabidopsis* protoplast using the polyethylene glycol-mediated transformation method⁵⁵. Alternatively, these constructs were also transiently expressed in onion epidermal cells using a particle gun-mediated system (PDS-1000/He; Bio-Rad). The transformed protoplasts and bombarded cells were held in the dark at 22 °C for more than 30 h followed by EYFP imaging using confocal microscopy (Olympus-FV1000).

For the GFP- or EYFP- fusion proteins expression in oocytes assay, the constructs were generated by introducing *NRT1.8-GFP*, *NPF5.11-EYFP*, *NPF5.12-EYFP* or *NPF5.16-EYFP* into the vector pOO2. The cRNA was synthesized and injected into oocytes. After cultivating 2 days, fluorescence was observed using confocal microscope (Olympus-FV1000).

Histochemical Analysis and Tissue Sectioning. A 1679-bp, a 1314-bp or a 1695-bp genomic fragment immediately upstream from the *NPF5.11*, *NPF5.12* or *NPF5.16* start codon, respectively, was amplified using primers listed in Supplemental Table S1. After sequencing, the fragments were cloned into the binary vector GUS/pCambia1300 and were then transformed into Col-0 as described³¹. GUS staining was performed overnight as described³¹. Semithin sections (4 μm) were cut, mounted on glass slides, and visualized on Leica-DM6000.

RT-PCR and Quantitative RT-PCR. Plants were grown to 28 days old in hydroponics, and then were sampled as indicated. Total RNA was extracted using TRIzol reagent (Invitrogen). First-strand cDNA synthesis and RT-PCR were performed as described³¹. Quantitative RT-PCR was performed on a Corbett Research Rotor-Gene 3000 thermal cycler using SYBR Premix Ex-Taq (TaKaRa) according to the manufacturer's protocol. The primers used in these assays are listed in Supplemental Table S1, and the expression levels were normalized to those of the *SAND* or *Actin2* control.

Nitrate Content Determination by HPLC. Plants were grown to 3–4 weeks old and were treated with nitrogen-starved nutrient solution for indicated time. Leaves and roots were harvested and washed at least three times by ultrapure water for 5 min and then extracted nitrate as described⁵⁶.

Analysis of Root-to-Shoot Nitrate Transport Using ¹⁵NO₃⁻. Wild type and triple mutant plants were grown in hydroponics for 28 days old and then were transferred to 0.1 mM CaSO₄ for 1 min, labeled in quarter-strength hydroponics medium with 2.25 mM K¹⁵NO₃ with 99% atom excess of ¹⁵N for 30 min. At the end of labeling, plants were washed in 0.1 mM CaSO₄ for 1 min and the shoots and roots were separated. The shoots and roots were sampled and detected as described⁵⁷.

Statistical Analysis. Two-tailed Student's *t* tests were performed. Differences were deemed significant (*) at $P < 0.05$ and extremely significant (**) at $P < 0.01$.

Data Availability. The datasets generated during and/or analyzed during the current study are available from the corresponding author on reasonable request.

References

1. Crawford, N. M. Nitrate: nutrient and signal for plant growth. *Plant Cell* **7**, 859–868 (1995).
2. Granstedt, R. C. & Huffaker, R. C. Identification of the leaf vacuole as a major nitrate storage pool. *Plant Physiol.* **70**, 410–413 (1982).
3. Martinoia, E., Heck, U. & Wiemken, A. Vacuoles as storage compartments for nitrate in barley leaves. *Nature* **289**, 292–294 (1981).

4. Cookson, S. J., Williams, L. E. & Miller, A. J. Light-dark changes in cytosolic nitrate pools depend on nitrate reductase activity in Arabidopsis leaf cells. *Plant Physiol.* **138**, 1097–1105 (2005).
5. Lea, U. S. *et al.* Mutation of the regulatory phosphorylation site of tobacco nitrate reductase results in high nitrite excretion and NO emission from leaf and root tissue. *Planta* **219**, 59–65 (2004).
6. Izmailov, S. F. Saturation and utilization of nitrate pools in pea and sugar beet leaves. *Russ J Plant Physiol.* **51**, 189–193 (2004).
7. van der Leij, M., Smith, S. J. & Miller, A. J. Remobilisation of vacuolar stored nitrate in barley root cells. *Planta* **205**, 64–72 (1998).
8. Martinoa, E., Maeshima, M. & Neuhaus, H. E. Vacuolar transporters and their essential role in plant metabolism. *J Exp Bot.* **58**, 83–102 (2007).
9. Krebs, M. *et al.* Arabidopsis V-ATPase activity at the tonoplast is required for efficient nutrient storage but not for sodium accumulation. *Proc Natl Acad Sci USA* **107**, 3251–3256 (2010).
10. Maeshima, M. Tonoplast transporters: organization and function. *Annu Rev Plant Physiol Plant Mol Biol.* **52**, 469–497 (2001).
11. Gaxiola, R. A., Palmgren, M. G. & Schumacher, K. Plant proton pumps. *FEBS Lett.* **581**, 2204–2214 (2007).
12. Schumacher, K. & Krebs, M. The V-ATPase: small cargo, large effects. *Curr Opin Plant Biol.* **13**, 724–730 (2010).
13. Miller, A. J. & Smith, S. J. Nitrate transport and compartmentation in cereal root cells. *J Exp Bot.* **47**, 843–854 (1996).
14. Kabala, K., Klobus, G. & Janicka-Russak, M. Nitrate transport across the tonoplast of *Cucumis sativus* L. root cells. *J Plant Physiol.* **160**, 523–530 (2003).
15. Miller, A. J. & Smith, S. J. The mechanism of nitrate transport across the tonoplast of barley root cells. *Planta* **187**, 554–557 (1992).
16. Schumacher, K. S. & Sze, H. Decrease of pH gradients in tonoplast vesicles by NO(3) and Cl: evidence for H-coupled anion transport. *Plant Physiol.* **83**, 490–496 (1987).
17. Sze, H. H⁺-translocating ATPases: advances using membrane vesicles. *Plant Biology* **36**, 175–208 (1985).
18. Blumwald, E. & Poole, R. J. Nitrate storage and retrieval in *Beta vulgaris*: Effects of nitrate and chloride on proton gradients in tonoplast vesicles. *Proc Natl Acad Sci USA* **82**, 3683–3687 (1985).
19. Geelen, D. *et al.* Disruption of putative anion channel gene AtCLC-a in Arabidopsis suggests a role in the regulation of nitrate content. *Plant J.* **21**, 259–267 (2000).
20. De Angeli, A. *et al.* The nitrate/proton antiporter AtCLCa mediates nitrate accumulation in plant vacuoles. *Nature* **442**, 939–942 (2006).
21. Chopin, F. *et al.* The Arabidopsis ATNRT2.7 nitrate transporter controls nitrate content in seeds. *Plant Cell* **19**, 1590–1602 (2007).
22. Lv, Q. *et al.* Cloning and molecular analyses of the Arabidopsis thaliana chloride channel gene family. *Plant Science* **176**, 650–661 (2009).
23. Harada, H., Kuromori, T., Hirayama, T., Shinozaki, K. & Leigh, R. A. Quantitative trait loci analysis of nitrate storage in Arabidopsis leading to an investigation of the contribution of the anion channel gene, AtCLC-c, to variation in nitrate levels. *J Exp Bot.* **55**, 2005–2014 (2004).
24. von der Fecht-Bartenbach, J., Bogner, M., Dynowski, M. & Ludewig, U. CLC-b-mediated NO₃/H⁺ exchange across the tonoplast of Arabidopsis vacuoles. *Plant Cell Physiol.* **51**, 960–968 (2010).
25. Hu, R. *et al.* Knock-down of a tonoplast localized low-affinity nitrate transporter OsNPF7.2 affects rice growth under high nitrate supply. *Front Plant Sci.* **7**, 1529 (2016).
26. Wege, S. *et al.* Phosphorylation of the vacuolar anion exchanger AtCLCa is required for the stomatal response to abscisic acid. *Sci Signal.* **7**, ra65 (2014).
27. Humble, G. D. & Hsiao, T. C. Specific requirement of potassium for light-activated opening of stomata in epidermal strips. *Plant Physiol.* **44**, 230–234 (1969).
28. Guo, F. Q., Young, J. & Crawford, N. M. The nitrate transporter AtNRT1.1 (CHL1) functions in stomatal opening and contributes to drought susceptibility in Arabidopsis. *Plant cell* **15**, 107–117 (2003).
29. Jaquinod, M. *et al.* A proteomics dissection of Arabidopsis thaliana vacuoles isolated from cell culture. *Mol Cell Proteomics* **6**, 394–412 (2007).
30. Tsay, Y. F., Chiu, C. C., Tsai, C. B., Ho, C. H. & Hsu, P. K. Nitrate transporters and peptide transporters. *FEBS Lett.* **581**, 2290–2300 (2007).
31. Li, J. Y. *et al.* The Arabidopsis nitrate transporter NRT1.8 functions in nitrate removal from the xylem sap and mediates cadmium tolerance. *Plant Cell* **22**, 1633–1646 (2010).
32. Tsay, Y. F., Schroeder, J. I., Feldmann, K. A. & Crawford, N. M. The herbicide sensitivity gene CHL1 of Arabidopsis encodes a nitrate-inducible nitrate transporter. *Cell* **72**, 705–713 (1993).
33. Schroeder, J. I. Physiology: nitrate at the ion exchange. *Nature* **442**, 877–878 (2006).
34. O'Brien, J. A. *et al.* Nitrate transport, sensing, and responses in plants. *Mol Plant.* **9**, 837–856 (2016).
35. Wang, C. *et al.* Rice SPX-Major Facility Superfamily3, a vacuolar phosphate efflux transporter, is involved in maintaining phosphate homeostasis in rice. *Plant Physiol.* **169**, 2822–2831 (2015).
36. Bergsdorf, E. Y., Zdebek, A. A. & Jentsch, T. J. Residues important for nitrate/proton coupling in plant and mammalian CLC transporters. *J Biol Chem.* **284**, 11184–11193 (2009).
37. Shen, J. *et al.* Organelle pH in the Arabidopsis endomembrane system. *Mol Plant.* **6**, 1419–1437 (2013).
38. Peng, J. S. & Gong, J. M. Vacuolar sequestration capacity and long-distance metal transport in plants. *Front Plant Sci.* **5**, 19 (2014).
39. Kataoka, T. *et al.* Vacuolar sulfate transporters are essential determinants controlling internal distribution of sulfate in Arabidopsis. *Plant Cell* **16**, 2693–2704 (2004).
40. Han, Y. L. *et al.* Nitrogen use efficiency is mediated by vacuolar nitrate sequestration capacity in roots of *Brassica napus*. *Plant Physiol.* **170**, 1684–1698 (2016).
41. Brunaud, V. *et al.* T-DNA integration into the Arabidopsis genome depends on sequences of pre-insertion sites. *EMBO Rep.* **3**, 1152–1157 (2002).
42. Scholl, R. L., May, S. T. & Ware, D. H. Seed and molecular resources for Arabidopsis. *Plant Physiol.* **124**, 1477–1480 (2000).
43. Alonso, J. M. *et al.* Genome-wide insertional mutagenesis of Arabidopsis thaliana. *Science* **301**, 653–657 (2003).
44. Sessions, A. *et al.* A high-throughput Arabidopsis reverse genetics system. *Plant Cell* **14**, 2985–2994 (2002).
45. Krysan, P. J., Young, J. C. & Sussman, M. R. T-DNA as an insertional mutagen in Arabidopsis. *Plant Cell* **11**, 2283–2290 (1999).
46. Mao, Y. *et al.* Application of the CRISPR-Cas system for efficient genome engineering in plants. *Mol Plant* **6**, 2008–2011 (2013).
47. Feng, Z. *et al.* Multigeneration analysis reveals the inheritance, specificity, and patterns of CRISPR/Cas-induced gene modifications in Arabidopsis. *Proc Natl Acad Sci USA* **111**, 4632–4637 (2014).
48. Gong, J. M., Lee, D. A. & Schroeder, J. I. Long-distance root-to-shoot transport of phytochelatin and cadmium in Arabidopsis. *Proc Natl Acad Sci USA* **100**, 10118–10123 (2003).
49. Ludewig, U., von Wiren, N. & Frommer, W. B. Uniport of NH₄⁺ by the root hair plasma membrane ammonium transporter LeAMT1;1. *J Biol Chem.* **277**, 13548–13555 (2002).
50. Hsu, P. K. & Tsay, Y. F. Two phloem nitrate transporters, NRT1.11 and NRT1.12, are important for redistributing xylem-borne nitrate to enhance plant growth. *Plant Physiol.* **163**, 844–856 (2013).
51. Huang, N. C., Liu, K. H., Lo, H. J. & Tsay, Y. F. Cloning and functional characterization of an Arabidopsis nitrate transporter gene that encodes a constitutive component of low-affinity uptake. *Plant Cell* **11**, 1381–1392 (1999).
52. Leran, S. *et al.* Arabidopsis NRT1.1 is a bidirectional transporter involved in root-to-shoot nitrate translocation. *Mol Plant* **6**, 1984–1987 (2013).

53. Lin, S. H. *et al.* Mutation of the Arabidopsis NRT1.5 nitrate transporter causes defective root-to-shoot nitrate transport. *Plant Cell* **20**, 2514–2528 (2008).
54. Wang, Y. Y. & Tsay, Y. F. Arabidopsis nitrate transporter NRT1.9 is important in phloem nitrate transport. *Plant Cell* **23**, 1945–1957 (2011).
55. Zhang, Y., Xu, Y. H., Yi, H. Y. & Gong, J. M. Vacuolar membrane transporters OsVIT1 and OsVIT2 modulate iron translocation between flag leaves and seeds in rice. *Plant J.* **72**, 400–410 (2012).
56. Meng, S. *et al.* Arabidopsis NRT1.5 mediates the suppression of nitrate starvation-induced leaf senescence by modulating foliar potassium level. *Mol Plant* **9**, 461–470 (2016).
57. Zhang, G. B., Yi, H. Y. & Gong, J. M. The Arabidopsis ethylene/jasmonic acid-NRT signaling module coordinates nitrate reallocation and the trade-off between growth and environmental adaptation. *Plant Cell* **26**, 3984–3998 (2014).

Acknowledgements

We thank Dr. Yi-Fang Tsay (Institute of Molecular Biology, Academia Sinica) for helping with electrophysiological analysis; Li Zhang (Instrumental Analysis Center, Shanghai Jiao Tong University) for helping with ¹⁵N analysis; and Xiao-Shu Gao (Core Facility, Shanghai Institute of Plant Physiology and Ecology, Shanghai Institutes for Biological Sciences) for helping with confocal microscopy. This work was supported by the National Science Foundation of China (Grants 31421093, 31325003) and the XDPB0402 of Chinese Academy of Sciences.

Author Contributions

J.G. and Y.H. designed the research. Y.H., Y.C., D.L., Y.G. and H.Y. performed the experiments. J.G., Y.H. and J.P. analyzed the data. J.G., Y.H. and J.P. wrote the paper.

Additional Information

Supplementary information accompanies this paper at doi:[10.1038/s41598-017-06744-5](https://doi.org/10.1038/s41598-017-06744-5)

Competing Interests: The authors declare that they have no competing interests.

Accession Codes: Sequence data from this article can be found in the Arabidopsis Genome Initiative or GenBank/EMBL databases under the following accession numbers: NPF5.11 (At1g72130), NPF5.12 (At1g72140), NPF5.16 (At1g22550), NRT1.8 (At4g21680), CHL1 (At1g12110), SAND (At2g28390), Actin2 (At3g18780).

Publisher's note: Springer Nature remains neutral with regard to jurisdictional claims in published maps and institutional affiliations.



Open Access This article is licensed under a Creative Commons Attribution 4.0 International License, which permits use, sharing, adaptation, distribution and reproduction in any medium or format, as long as you give appropriate credit to the original author(s) and the source, provide a link to the Creative Commons license, and indicate if changes were made. The images or other third party material in this article are included in the article's Creative Commons license, unless indicated otherwise in a credit line to the material. If material is not included in the article's Creative Commons license and your intended use is not permitted by statutory regulation or exceeds the permitted use, you will need to obtain permission directly from the copyright holder. To view a copy of this license, visit <http://creativecommons.org/licenses/by/4.0/>.

© The Author(s) 2017